Experimental fine-structure branching ratios for Na—rare-gas optical collisions

M. D. Havey, F. T. Delahanty, L. L. Vahala, and G. E. Copeland
Physics Department, Old Dominion University, Norfolk, Virginia 23508
(Received 22 May 1986)

Experimental ratios for branching into the fine-structure levels of the Na $3p$ multiplet, as a consequence of an optical collision with He, Ne, Ar, Kr, or Xe, are reported. The process studied is $\mathrm{Na}(3s\,^2S_{1/2})+\mathscr{R}+nh\nu\rightarrow\mathrm{Na}(3p\,^2P_j)+\mathscr{R}+(n-1)h\nu$, where $\mathscr{R}$ represents a rare-gas atom and where the laser frequency ν is tuned in the wings of the Na resonance transitions. The branching ratios are defined as $I(D1)/I(D2)$ where $I(D1)$ and $I(D2)$ are measured intensities of the atomic Na $D1$ and $D2$ lines. The ratios are determined for detunings ranging from about 650 cm^{-1} in the blue wing to 170 cm^{-1} in the red wing of the Na $3p$ multiplet. The branching is found to be strongly detuning dependent in the vicinity of the NaAr, NaKr, and NaXe near-red-wing satellites. The blue-wing branching ratios show a detuning-dependent approach to a recoil, or sudden statistical, limit of 0.5, irrespective of the rare gas. Fine-structure changing cross sections have also been measured for resonant excitation of the Na $3p\,^2P_j$ state; the results are consistent with cross sections obtained from wing excitation.

I. INTRODUCTION

Nonadiabatic couplings among states of a colliding pair of atoms or molecules have an essential role in determining state-specific cross sections for a wide range of elastic and inelastic collision processes.[1–17] These include nonradiative electronic transitions such as quenching or fine-structure transitions, coherence transfer, and rotational and vibrational energy transfer. Nonadiabatic effects are also important in photofragmentation processes such as photodissociation,[16] photoionization,[17] or collisional redistribution of light.[5,12,13] For these and other fragmentation processes, normally small nonadiabatic couplings can exert considerable influence on the dynamics in the vicinity of curve crossings among the molecular terms of the system. However, for systems dissociating to degenerate or nearly degenerate atomic or molecular states there is, in addition, a range of fragment separations for which the nonadiabatic couplings are comparable to the interfragment potentials.[16] For example, in a heteronuclear van der Waals diatomic molecule the long-range potentials fall off typically as fast as R^{-6}, while rotational mixing[18] of the Born-Oppenheimer terms[19] decreases as R^{-2} and comes to dominate the long-range interatomic interactions. The rotational nonadiabaticity has a profound effect on the polarization of light emitted from excited atoms produced in optical collisions, as recent experiments on group-II—rare-gas-atom collisions have shown.[1,2,5,12,13]

In this paper we are concerned with optical collisions between atoms having fine structure and thus for which nonadiabatic effects due to the spin-orbit and rotational interactions can be important. As the spin-orbit Hamiltonian[19] is nondiagonal in a Hund's case (a) basis (which may be used to define adiabatic Born-Oppenheimer potentials), consideration of these cases necessarily leads to strong nonadiabatic effects among the excited adiabatic molecular terms as the atoms separate to their asymptotic fine-structure states.

We report here on our studies[20] of the process

$$\mathrm{Na}(3s\,^2S_{1/2})+\mathscr{R}+nh\nu\rightarrow\mathrm{Na}(3p\,^2P_j)+\mathscr{R}+(n-1)h\nu\ , \tag{1}$$

where $\mathscr{R}$ represents He, Ne, Ar, Kr, or Xe and where $nh\nu$ represents a radiation field of frequency ν having n photons. The frequency ν is tuned in to the wings of the Na $D1$ and $D2$ lines. We have measured for process (1) the branching into each of the Na $3p\,^2P_j$ fine-structure levels for a detuning ranging from 650 cm^{-1} in the blue wing to about 170 cm^{-1} in the red wing of the Na $3p$ multiplet. Strong nonadiabatic effects are apparent in the data. We have also determined, for all the rare gases, the cross sections for population transfer $[\mathrm{Na}(^2P_{1/2})+\mathscr{R}\rightarrow\mathrm{Na}(^2P_{3/2})+\mathscr{R}]$ within the Na $3p$ fine-structure multiplet. The cross sections are measured for both resonant and far-wing excitation of the $3p$ states.

The remainder of this paper is organized as follows. In the next section we discuss briefly the basic process (1). This is followed by a detailed description of our experimental apparatus and methodology. We then present and discuss our experimental branching-ratio data and the results of our measurements of fine-structure population transfer cross sections.

II. EXPERIMENT

The experimental scheme we use to study process (1) is illustrated[21] in Fig. 1. In this scheme an optically thin gaseous mixture of Na and low-density rare-gas atoms is illuminated by laser radiation tuned into the far wings of the collisionally perturbed Na resonance transitions. We define the detuning Δ to be $\nu-\nu(D2)$ ($\Delta>0$) for laser frequencies ν higher than that of the Na $D2$ transition and to be $\nu-\nu(D1)$ ($\Delta<0$) for ν lower than the Na $D1$ transition. Thus, excitation when $\Delta\gg0$ corresponds mainly

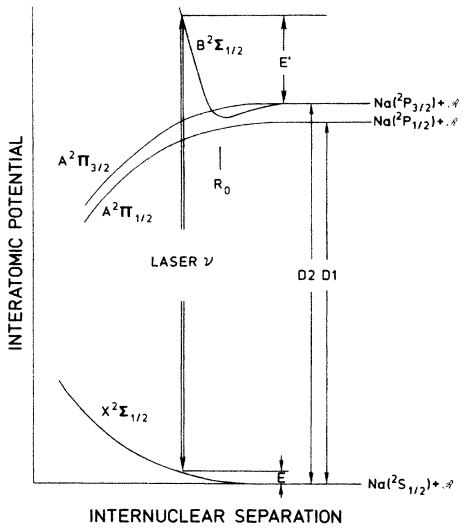

FIG. 1. Qualitative potentials for the lowest three states of Na$\mathscr{R}$ molecules.

to free-free molecular transitions between the $X\,^2\Sigma_{1/2}$ and $B\,^2\Sigma_{1/2}$ states, while excitation for $\Delta \ll 0$ corresponds to free-free and free-bound transitions between the $X\,^2\Sigma_{1/2}$ and the $A\,^2\Pi_{1/2,3/2}$ states. To illustrate the experimental scheme we discuss the case $\Delta \gg 0$.

Consider a collision, with total center-of-mass energy E, between a Na and a rare-gas atom along the $X\,^2\Sigma_{1/2}$ potential $V_x(R)$. The collision is supposed to occur in a linearly polarized laser field of frequency ν. If transitions are to occur we must have $h\Delta = E' - E$. The classical Franck-Condon principle[22] then implies $h\Delta = V_b(R) - V_x(R)$. For a monotonic difference potential, $V_b(R) - V_x(R)$, transitions occur at a particular internuclear separation R; this selects a range of impact parameters 0 to R. Following excitation, the Na$\mathscr{R}$ molecule dissociates initially in the $B\,^2\Sigma_{1/2}$ state. As the Na$\mathscr{R}$ separation nears R_0, spin-orbit and rotational interactions[18] cause transitions among the molecular case (a) states. As these molecular states correlate to the two ^2P_j states, there is some likelihood that the molecule will dissociate into the $^2P_{1/2}$ or $^2P_{3/2}$ state. Furthermore, experiments[23] and calculations,[23,24] have indicated that dissociation will be into a nonuniform distribution of atomic Na m_j states. To determine experimentally the relative cross sections for scattering into the two fine-structure states, the relative intensity of the resulting Na emission lines, $I(^2P_{3/2} - {}^2S_{1/2})$ $[I(D2)]$ and $I(^2P_{1/2} - {}^2S_{1/2})$ $[I(D1)]$ are measured. These intensity measurements define, in the limit of zero rare-gas density, a branching ratio $B(\Delta)$ according to $B(\Delta) = I(D1)/I(D2)$. As $\nu(D1)/\nu(D2) = 0.999$, $B(\Delta)$ is essentially the ratio of the populations produced in the Na $3p$ fine-structure states. For the Na-$\mathscr{R}$ systems in our experimental geometry, the spatial anisotropy of the $D2$ emission resulting from the m_j dependence of process (1) has a minor effect on $I(D2)$ (see the following section). For a linearly polarized radiation field, there is no effect on $I(D1)$. The m_j dependence of (1) may be studied by measurements of the polarization of the emission lines;[23] our main concern here is with the fine-structure branching.

A schematic diagram of our experimental apparatus is shown in Fig. 2. In the scheme of Fig. 2, the vertically polarized output of an Ar^+-laser-pumped ring dye laser is tuned in to the wings of the collisionally perturbed Na resonance lines. The dye-laser output is passed through a 12-cm-long Na absorption cell operating at 150°C and containing about 270 torr of Ar. The cell removes, from the laser output, amplified spontaneous emission at the Na D lines; this portion of the emission otherwise would excite the Na atoms resonantly, generating a signal comparable to that from wing excitation by the main laser output. The ring laser generated about 500 mW in a bandwidth of approximately 1 cm^{-1}; focusing the laser output into the central portion of the sample cell produced a power density of about 1 kW/cm^2 there. Note that this is a weak field for far-wing excitation, as confirmed by the linearity of the fluorescence signals with laser intensity variations. There was also no measurable effect of laser intensity on the branching ratios. The beam was multiply passed through and focused into the cell by means of two spherical mirrors. The reflected beams did not overlap in the interaction region. With this

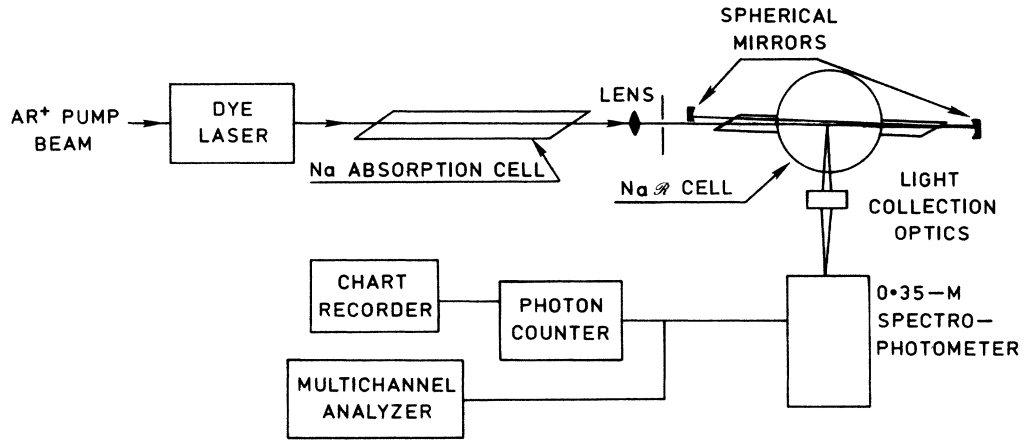

FIG. 2. Schematic diagram of the experimental apparatus.

arrangement wing signals were increased typically eight times over those from a single beam.

A description of the Na-$\mathscr{R}$ cell and its operation has been presented previously;[25] for the experiments described here the cell-generated Na densities in the range 10^9–10^{11} cm^{-3} at a cell temperature of about 303 K. The cell was connected to an oil-free vacuum-gas handling system, facilitating rapid gas and gas pressure changes. The base cell pressure was about 10^{-7} torr. Rare gas pressures were typically in the range 0–5 torr. Research-grade rare gases were used in all experiments with no further purification.

The Na $D1$ and $D2$ fluorescence was detected at right angles to the laser beam and its polarization vector. Fluorescence was gathered by $f/6$ optics and focused with unit magnification onto the slits of a 0.3-m monochromator, which had a spectral resolution of around 0.2 nm. The monochromator throughput was detected by an S-20 cathode photomultiplier tube (PMT) operated in a photon-counting mode. The cooled PMT had a dark counting rate of about 1 Hz; maximum fluorescence signals were about 20000 Hz. As the monochromator was scanned over the D lines, the photon-counting signal was processed and displayed on a chart recorder. The ratio of the peak intensities R provided a measure of the relative populations produced in the Na $3p\,^2P_j$ states. Auxiliary experiments were performed in which the signals were stored in a synchronously scanned multichannel analyzer and the ratio of the integrated line intensities provided the measure of the relative populations produced in the Na $3p\,^2P_j$ states. There were no measurable differences between the results. The spectral response of the systems was flat over the D lines. This was confirmed by measuring R with 100-torr He in the cell. Under these circumstances the D-line emission is virtually unpolarized and R should be nearly equal to its thermal equilibrium value of 0.543; this was confirmed to within an experimental uncertainty of 2%.

III. RESULTS AND DISCUSSION

A. Systematic effects

In general, when the laser frequency was tuned into the Na D-line wings we observed emission only at the Na D lines. No other emission was observed throughout the visible and near visible, including atomic Na transitions that terminate in the $3p$ state and the $4p$-$3s$ second resonance transition. Our measurements, then, consisted of determination of the relative intensities of the D lines measured as a ratio R. Variations in the laser intensity over a factor of 5 showed the individual D-line intensities to increase linearly with laser intensity; the ratio R was independent of that quantity. The sum of the intensities depended linearly on the rare-gas pressure, as expected for unsaturated wing excitation. The ratio R of these intensities may, however, be systematically distorted by several physical effects.

First, the measured ratio depends on the pressure of the rare gas. The pressure dependence is due to fine-structure changing collisions that occur after far-wing absorption and dissociation, but prior to radiative decay of the Na $3p$ states. A straightforward rate-equation analysis of the pressure dependence yields

$$R=[B(\Delta)+I_\infty xP]/(1+xP)\,, \tag{2}$$

where R is the measured branching ratio at rare-gas pressure P, $B(\Delta)$ the limit of R when $P\to 0$, and where I_∞ is the thermal equilibrium ($P\to\infty$) limit of R; $I_\infty=\frac{1}{2}e^{\Delta E/kT}$ with ΔE the atomic Na fine-structure splitting of 17.3 cm^{-1}. The quantity x is $(K_{12}/\gamma)[1+B(\Delta)]$, K_{12} being the rate constant for collisional $^2P_{1/2}\to{}^2P_{3/2}$ transitions and γ the radiative decay rate of the Na $3p$ states[26] ($\gamma=6.13\times10^7$ s^{-1}). Equation (2) may be put in alternate forms linear in P:

$$R=B(\Delta)-(R-I_\infty)xP \tag{3a}$$

or

$$(R-I_\infty)^{-1}=[B(\Delta)-I_\infty]^{-1}(1+xP)\,. \tag{3b}$$

To account for the pressure dependence, we generally measured R as a function of P for 0.5-torr increments in the range 0–5 torr and did a least-squares fit of the data to Eqs. (2) and (3), extracting x and $B(\Delta)$ from the slope and intercept of the fit. It is these quantities that are the basic results of our experiments. The quality of the fit is demonstrated by the NaXe data in Fig. 3. Each point is obtained from the average result of three scans over the D lines, and the error bars represent the statistical uncertainty (mainly due to photon counting statistics) in R. For all of the data, except those for He, the three fitting methods yielded values of $B(\Delta)$ within the combined statistical uncertainties in the fits (10–15%). For that case, however, the $B(\Delta)$ values are all near I_∞ and the fine-structure mixing rate is large; the resulting fit-to-fit variations were about 25%. Improving on this would require that data be taken for pressures below 0.5 torr; our present signal-to-noise ratio does not allow meaningful data to be taken there.

Branching ratios for NaHe were obtained by extrapolating to $P=0$ values of R measured at 1.0 and 0.5 torr. The value of K_{12} used in the extrapolation was that mea-

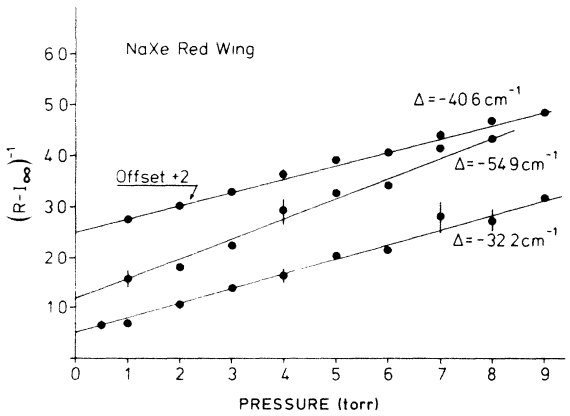

FIG. 3. Measured pressure dependence of $(R-I_\infty)^{-1}$ for several detunings in the NaXe red-wing satellite region. Data are presented from 9 torr to illustrate the good quality of least-squares fits to Eq. (3), represented by the solid lines.

sured for resonant excitation of the Na D lines under the same experimental conditions as our wing excitation measurements. The details of the K_{12} measurements are presented in Sec. III C.

For all the other rare gases, there were generally small systematic differences in the values of $B(\Delta)$ obtained from the three fits. Except for values of R near I_∞, the differences were within the combined uncertainties in the fits. For these values Eq. (3b) was unsuitable because the quantity $(R-I_\infty)^{-1}$ magnifies small measurement errors in R. Fits to Eq. (3a) showed the least sensitivity to small errors in R, and the $B(\Delta)$ data reported here are from that fit.

Note that, for all the NaR molecules except NaNe, the $A\,\Pi$ state shows binding substantially greater[27-29] than kT. This means that for red detunings on the order of kT an additional pressure dependence (and systematic effect) can originate from excitation of free-bound $X\Sigma - A\,\Pi$ transitions followed by collisional dissociation of the $A\,\Pi$ state into free Na atoms. For this reason, we limit our red detunings to be less than 170 cm^{-1}, for which approximately 65% of the excitation is to free scattering states.

Second, radiation trapping[30] of the Na resonance radiation may effect R. The absorption coefficient for $D2$ radiation is twice that for $D1$ radiation, and so radiation trapping may increase the measured value of R. However, our measurements of R showed no sensitivity to variations of [Na] over a factor of 10, measured by the size of the total Na resonance fluorescence signal.

Third, as a result of wing excitation with linearly polarized light the Na $^2P_{3/2}$ state may be aligned; the $^2P_{1/2}$ state will support no alignment. The resulting $^2P_{3/2}\rightarrow{}^2S_{1/2}$ $D2$ emission has the following angular distribution:[31]

$$I(\theta)=I_0/4\pi[1+\tfrac{5}{8}A_0'P_2(\cos\theta)]\ . \tag{4}$$

I_0 is the total spatially integrated $D2$ emission and $P_2(\cos\theta)$ the second Legendre polynomial. The angle between the polarization vector of the exciting light and the detector axis is θ. The alignment[32] A_0' may be written as $A_0'=g^{(2)}A_0$, where A_0 is the alignment produced by wing excitation and dissociation and where $g^{(2)}=0.29$ accounts for the depolarizing influence of the $^2P_{3/2}$-state hyperfine structure. For our experimental geometry $\theta=90°$, and for a maximum $^2P_{3/2}$ alignment of $A_0=-0.8$, $I(D2)$ is 7.2% larger than it would be for isotropic emission. Theoretical[23,24] and experimental[23] results for NaAr and experimental data[1,2,5,12,13] on the group-II–rare-gas systems show considerably less alignment than the maximum. For NaAr the maximum calculated alignment from blue-wing excitation[24] is about $A_0=-0.32$, with a resulting maximum decrease in B of about 3%. These numbers are considerably smaller than our statistical uncertainties in $B(\Delta)$ and we have thus made no corrections to the data for this effect. The rare-gas pressure dependence of A_0' (due to disaligning collisions) thus is not included in the rate equations [Eqs. (2) and (3)] describing the pressure dependence of R. Note that the effect of alignment on $B(\Delta)$ may be removed by using a linear polaroid, in the detection optics, tilted at the magic angle of 54.7° from the vertical. However, the removal of the small systematic effect due to A_0' is superceded by the resulting decreased (about 1.4) signal-to-noise ratio.

Finally, the effect of the hyperfine structure on the angular momentum dynamics should be negligible for free-free scattering; the hyperfine precession frequencies are all much smaller than a typical inverse collision time. The initially unpolarized nuclear spin is thus brought to the final atomic states, and its effect accounted for by $g^{(2)}$. In a long-lived excited-state scattering resonance or quasi-bound state the alkali-metal and the rare-gas nuclear spins may significantly couple to the initially aligned electronic angular momentum. However, theoretical calculations[24] show that such resonances may play a significant role in the optical collision only for far-red-wing detunings. They should have a minor effect on the branching-ratio measurements reported here. Their effect on polarization measurements, however, may be significant.

B. Branching-ratio results and discussion

Our results for the red- and blue-wing branching ratios $B(\Delta)$ for all the Na$\mathscr{R}$ pairs are presented in Figs. 4 and 5. Except as discussed in Sec. III A, each data point represents $B(\Delta)$ obtained from a fit of the data to Eq. (3a). As discussed in Sec. III A, the error bars on $B(\Delta)$ represent the uncertainty in $B(\Delta)$ due to photon counting statistics and due to the extrapolation of measured values of R to zero pressure. The uncertainty in Δ is on the order of 2 cm^{-1}, depending upon detuning, and is due to the limited spectrometer resolution. Comparisons of the NaHe, NaNe, and NaAr data with available theoretical calculations are made in Ref. 24, where it is seen that the overall agreement is quite good.

In general, we see from the figures strong variations in $B(\Delta)$ with rare gas and with detuning, indicating that the interatomic potentials play an important role in determining $B(\Delta)$. Furthermore, adiabatic correlation would predict $B(\Delta)=0$ for $\Delta\gg0$ and $B(\Delta)=1$ for $\Delta\ll0$. The behavior of $B(\Delta)$ in Figs. 4 and 5 then indicates that strong nonadiabatic mixing must be taking place among the Na$\mathscr{R}$ molecular terms.

Consider first the blue-wing results. For $\Delta\gg0$ we see that $B(\Delta)$ for NaHe and NaNe has closely approached a common limit of 0.5. As discussed by Singer *et al.*[16] such a recoil, or sudden statistical, limit is expected to be obtained whenever the dissociation is fast compared to an inverse fine-structure coupling frequency.[16,24] As dissociation occurs with higher velocity for the lighter Na$\mathscr{R}$ molecules and for larger Δ, we expect to approach this limit more closely for large detunings and for lighter molecules; the data for all the Na$\mathscr{R}$ molecules support this expectation. However, in the near blue wings we see considerable variation in $B(\Delta)$, and that the recoil limit is approached from below 0.5 for NaHe and NaNe, but from above 0.5 for NaAr, NaKr, and NaXe. We believe this behavior to be due to the considerable $B\Sigma$ binding for the heavier Na$\mathscr{R}$ molecules,[33] resulting in a strong $B\,^2\Sigma_{1/2}-A\,^2\Pi_{1/2}$ coupling in the vicinity of the $B\Sigma$ potential minimum. To see this, consider that blue-wing excitation produces primarily the Na$\mathscr{R}$ $B\,^2\Sigma_{1/2}$ state. Diabatic passage through the localized $B\,^2\Sigma_{1/2}-A\,^2\Pi_{1/2}$ curve crossing converts this to the $A\,^2\Pi_{1/2}$ state which

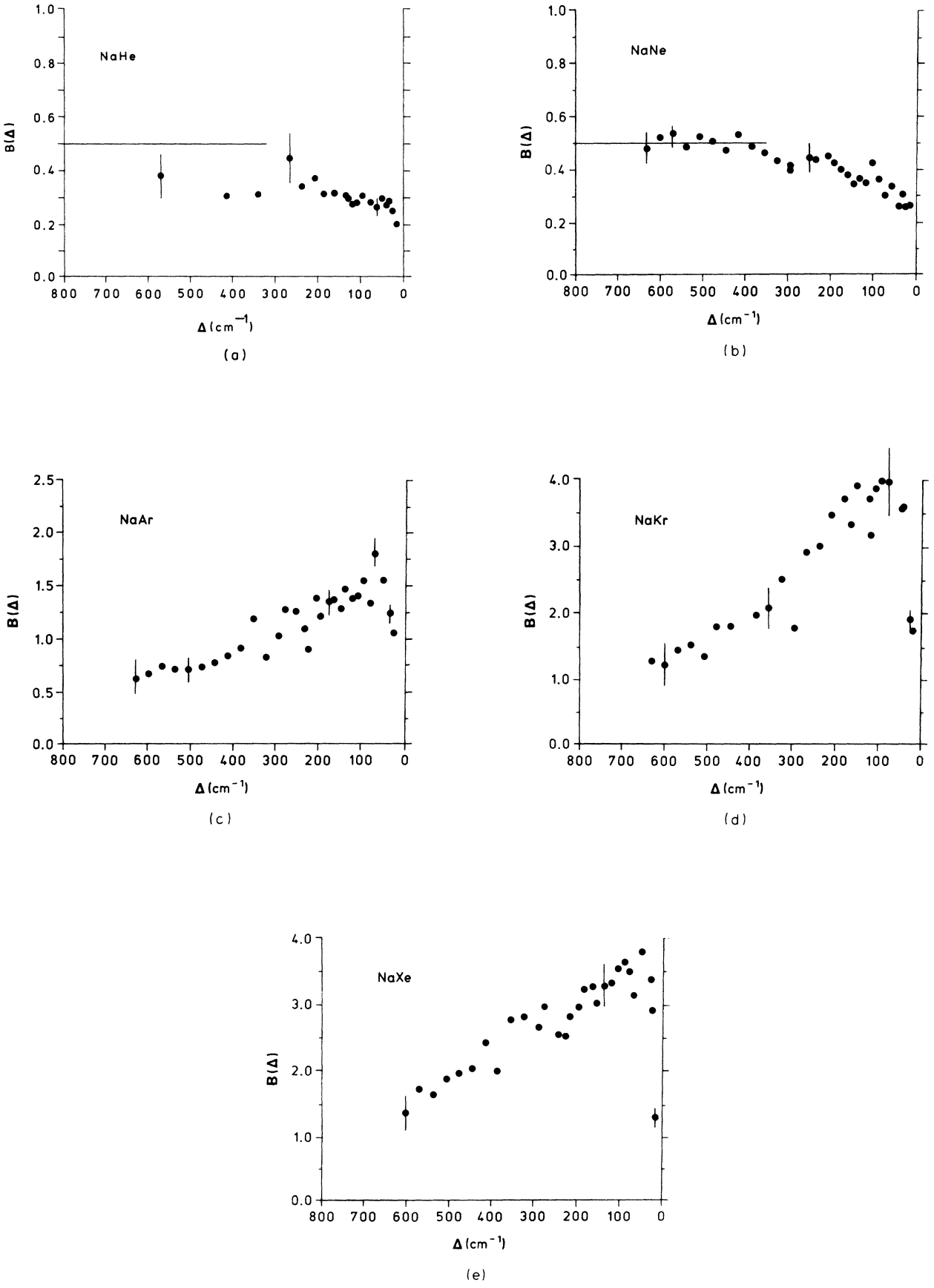

FIG. 4. Branching ratios $B(\Delta)$ vs Δ for the Na$\mathscr{R}$ blue wings. (a) NaHe, (b) NaNe, (c) NaAr, (d) NaKr, (e) NaXe.

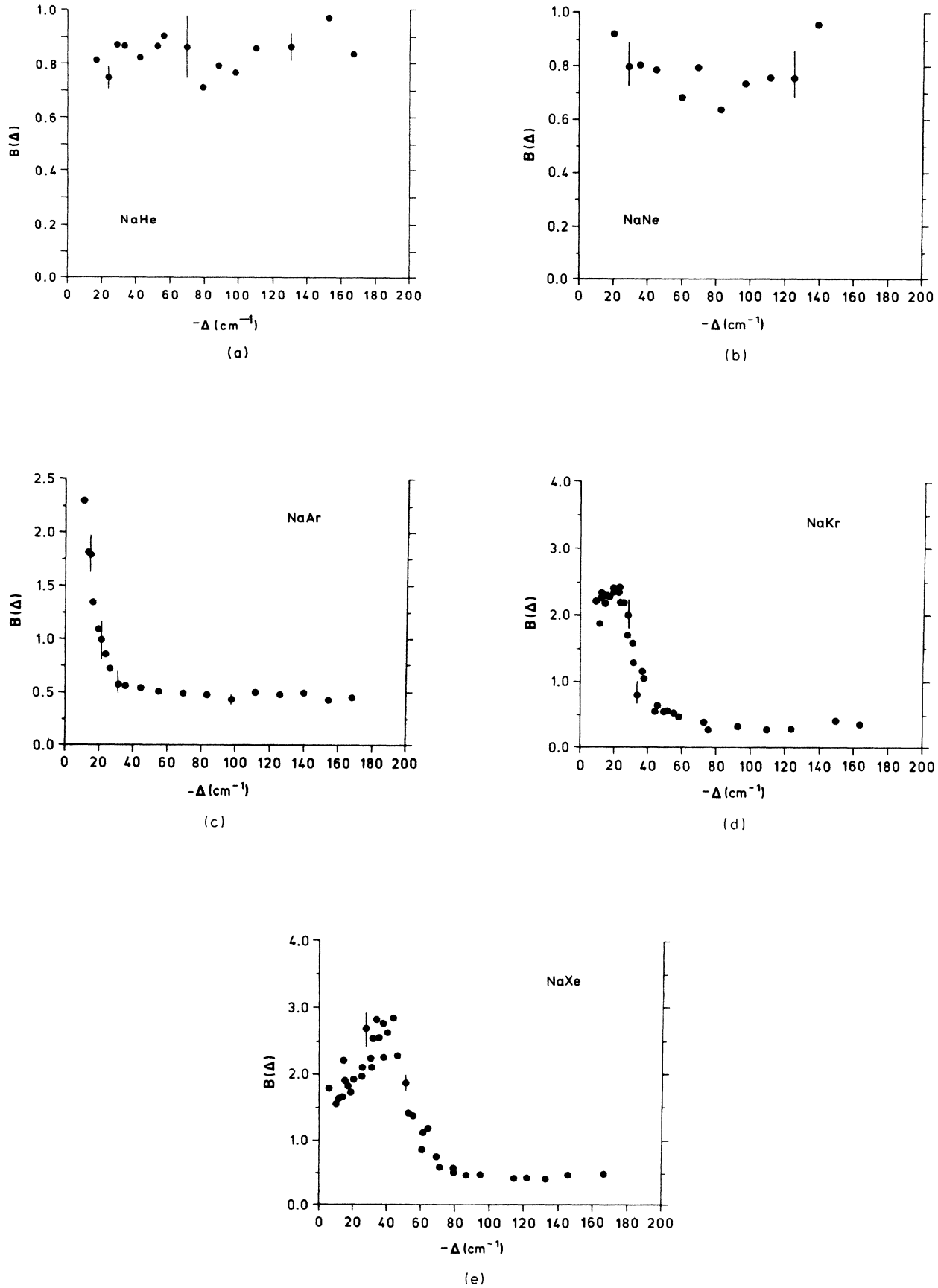

FIG. 5. Branching ratios $B(\Delta)$ vs Δ for the Na$\mathscr{R}$ red wings. (a) NaHe, (b) NaNe, (c) NaAr, (d) NaKr, (e) NaXe.

correlates adiabatically to the Na $^2P_{1/2}$ state. Since rotational mixing of the $A\,^2\Pi_{1/2}$ into the $A\,^2\Pi_{3/2}$ and $B\,^2\Sigma_{1/2}$ states is weak, compared to the size of the spin-orbit coupling, dissociation into the $^2P_{1/2}$ state should be favored, and we see from the data that it is. The branching ratios then should approach the recoil limit from above 0.5 for systems with $B\,^2\Sigma_{1/2}$ binding comparable to the fine-structure splitting. For NaHe and NaNe, reliable potentials[34,35] show the $B\,^2\Sigma_{1/2}$ binding to be considerably less than the spin-orbit coupling and so $B(\Delta)$ should, according to this qualitative model, approach 0.5 from below; we see that indeed it does. Note that full close-coupled case-(a) wave functions[24] for NaAr optical collisions indeed show the diabatic $B\,^2\Sigma_{1/2}\rightarrow A\,^2\Pi_{1/2}$ behavior just discussed. Finally, near-resonant $D2$ excitation should produce a very small $B(\Delta)$; the branching ratio indeed decreases sharply in the near blue wings.

In the far red wings ($\Delta \ll 0$) we see in the data a situation complimentary to that described in the previous paragraph. For the red wings, optical excitation is primarily to the $A\,^2\Pi_{3/2}$ and $A\,^2\Pi_{1/2}$ states, with relative strengths given roughly by, and for van der Waals wings, $[\Delta/(\Delta+17.3)]^{3/2}$. We then expect, for NaHe and NaNe (which have no strong $B\,^2\Sigma_{1/2}-A\,^2\Pi_{1/2}$ curve crossing) that $B(\Delta)$ will be less than 1, but above the recoil limit of 0.5. For NaAr, NaKr, and NaXe, on the other hand, the strong diabatic curve crossing converts most of the $A\,^2\Pi_{1/2}$ amplitude created by optical excitation to $B\,^2\Sigma_{1/2}$, making $B(\Delta)$ small. Note, for large red-wing detunings, we do not approach a recoil limit; this is due to the decrease in the average E' with increasing Δ.

In the near red wings we see striking satellites in the NaAr, NaKr, and NaXe branching ratios. Corresponding satellites[36,37] in the total absorption coefficient have been known for some time and are generally thought to have their origin in an extremum in a ground-state—excited-state difference potential. A possible origin for the satellites seen here assumes that they are due to an extremum in the $X\,^2\Sigma_{1/2}-A\,^2\Pi_{1/2}$ (see Fig. 1) difference potential; excitation then produces mainly the $A\,^2\Pi_{1/2}$ state. The favoring of the $^2P_{1/2}$ state may then be understood as nearly adiabatic dissociation to the $^2P_{1/2}$ state.

For detunings within the impact limit direct excitation of the $^2P_{1/2}$ state should dominate wing excitation of the $^2P_{3/2}$ state and as a result $B(\Delta)$ should be very large. However, our data do not extend into this region, and they thus do not show this limit.

To summarize our branching-ratio results, we see in the far blue wings an approach to a recoil limit irrespective of the rare gas; for NaHe and NaNe this limit has been closely approached. In the near blue wings significant departures from a recoil limit are measured, indicating strong potential and spin-orbit effects on $B(\Delta)$. For NaKr at $\Delta=100$ cm^{-1}, for example, nearly 80% of the excited Na atoms produced are in the $^2P_{1/2}$ state, the state of lower statistical weight. In the near red wings, pronounced $B(\Delta)$ satellites are observed for NaAr, NaKr, and NaXe; they are likely due to an extremum in the $X\,^2\Sigma_{1/2}-A\,^2\Pi_{1/2}$ difference potentials. In the far red wings $B(\Delta)$ complements the near-blue-wing data, indicating that a strong diabatic $B\,^2\Sigma_{1/2}-A\,^2\Pi_{1/2}$ transition

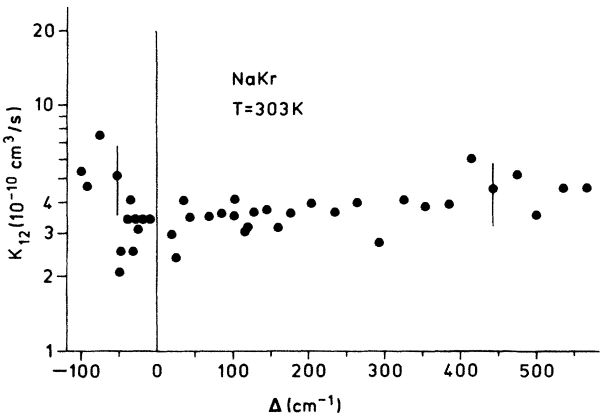

FIG. 6. Fine-structure transition rate constant $K_{12}(\Delta)$ vs Δ for NaKr. Data with a correlation coefficient of 0.6 or higher are shown in the figure.

occurs for NaAr, NaKr, and NaXe, but not for NaHe and NaNe. The essential determinants of $B(\Delta)$ then appear to be the detuning-dependent mixture of states produced by optical excitation and the presence or absence of a well-defined curve crossing in the $B\,^2\Sigma_{1/2}-A\,^2\Pi_{1/2}$ potentials. Rotational mixing appears to play a lesser role.

C. Fine-structure mixing rates

As a result of fitting the R versus P data to Eqs. (2) and (3), values for the fine-structure mixing rate constant K_{12} were determined along with $B(\Delta)$. Our NaKr data are displayed in Fig. 6. The values so determined have considerable uncertainty (20—30%), as they depend on both the slope and intercept of the linear fits. Nevertheless, K_{12} is found to be constant (within the uncertainty) in the near red and blue wings for all rare gases, but to increase slightly in the far blue wings for NaKr and NaXe. An increase in K_{12} for greater blue-wing detunings is not unexpected; increasing Δ leads to a higher Na-atom speed

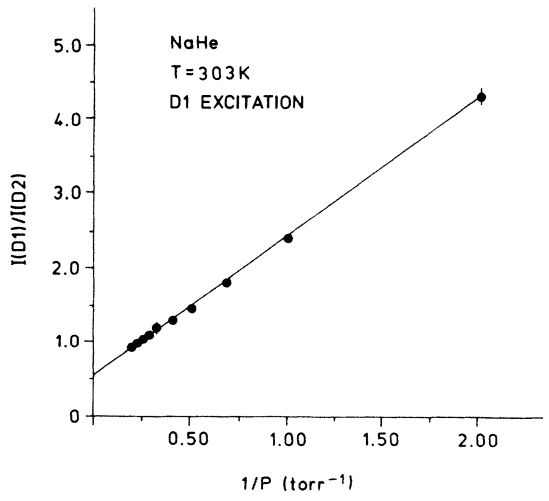

FIG. 7. Pressure dependence of $I(D1)/I(D2)$ for resonant excitation of the Na $D1$ line. The solid line is a least-squares fit of the data to Eq. (5).

TABLE I. Comparison of fine-structure transition rate constants determined from this work and determined by others. The value of I_∞ at $T=303$ K is 0.543. The rate coefficients at $T=400$ K are taken from Ref. 38. The values in parentheses denote the uncertainty in the last digits.

Species	K_{12} (10^{-10} cm^3/s) nonresonant	K_{12} (10^{-10} cm^3/s) resonant $T=303$ K	I_∞ resonant $T=303$ K	K_{12} (10^{-10} cm^3/s) $T=400$ K
NaHe		10(1)	0.54(5)	
NaNe	5.2(2.4)	5.0(5)	0.59(6)	7.5(2.5)
NaAr	5.0(8)	6.3(6)	0.57(5)	10.7(1.3)
NaKr	3.7(7)	4.2(4)	0.60(6)	8(2)
NaXe	3.1(6)	4.8(5)	0.57(4)	7(1)

upon dissociation, and K_{12} is known to increase[38] with velocity in the range associated with our blue-wing data. Furthermore, the results of Liao *et al.*[39] show that the higher Na speeds should show some persistence, despite subsequent fine-structure changing collisions. In our experiments the better signal-to-noise and larger branching ratios, along with the larger rare-gas mass, make observation of this effect most favorable for NaKr and NaXe. The velocity dependence of K_{12} is also more rapid for those gases in the range of effective velocities accessible to our experiments.

The average near-wing K_{12} values are somewhat smaller than one would expect by extrapolating existing data[38] on the velocity dependence of K_{12} to our average thermal energy ($kT=210$ cm^{-1}). We have therefore measured, by resonant excitation, the fine-structure mixing rates for all the Na$\mathscr{R}$ pairs at a cell temperature of about 303 K. In these experiments, the $D1$ line was resonantly excited with linearly polarized light attenuated to an intensity of about 1 W/cm^2. The multimode laser excitation did not saturate the resonant excitation under these conditions. The rate constant was determined, as for wing excitation, from the pressure dependence of $I(D1)/I(D2)$. A simple rate-equation model of this ratio yields

$$I(D1)/I(D2)=I_\infty+\gamma/K_{12}P\ . \tag{5}$$

Our data were described very well by Eq. (5), as the NaHe results in Fig. 7 show. Note that coherence transfer to the $^2P_{3/2}$ state [which would make, as per Eq. (4), $I(D2)$ systematically in error] is negligible in our experiment. All results were independent of Na density, laser power and yielded values of I_∞ within 10% of the detailed balance value of 0.543.

Our results for K_{12} and I_∞ are summarized in Table I, where they are compared with the average value obtained from near-wing (± 200 cm^{-1}) excitation. No wing-excitation data for NaHe are presented; $B(\Delta)$ is near I_∞ for all data, making the pressure dependence weak [Eq. (2)] and K_{12} very poorly determined. For the other cases, the values of K_{12} determined from wing excitation are generally smaller than those found by resonant excitation, but, except for NaXe, within the combined error bars of the measurements. For comparison purposes we also list in Table I the values of K_{12} obtained by Apt and Pritchard[38] at $T=400$ K for NaNe, NaAr, NaKr, and NaXe. For these cases we see that K_{12} at $T=400$ K is substantially larger than K_{12} at $T=303$ K. This implies a strong increase of K_{12} with temperature in this range. We have confirmed that K_{12} in fact increases towards the $T=400$ K value by measuring the rate coefficient for NaXe at $T=370$ K; we obtain the intermediate value of $5.7(7)\times 10^{-10}$ cm^3/s at this temperature.

Finally, we note that values for I_∞ for NaHe, NaNe, NaAr, and NaKr were determined directly from the intercept of fits to Eq. (5). Small amounts of scattered laser light make these values systematically large by a few percent; no corrections were made for this effect. For NaXe, I_∞ was determined directly from the ratio of measured rate coefficients K_{12}/K_{21}; K_{21} was determined from the pressure dependence of $I(D2)/I(D1)$ with $D2$-line excitation. For these measurements a magic-angle polaroid (see Sec. III A) in the detection arm removed systematic effects associated with alignment of the $^2P_{3/2}$ state. Within our experimental uncertainty, I_∞ so determined is in agreement with the value expected from detailed balance.

IV. CONCLUSIONS

We have experimentally determined fine-structure branching ratios for Na$\mathscr{R}$ optical collisions. The measurements show a strong sensitivity to the interatomic potentials and to nonadiabatic effects in the dissociation dynamics, provided that the final-state scattering energy is not too large. With increasing dissociation velocity we see the branching ratio approach a recoil limit of 0.5 which is independent of the rare gas. The approach to the limit from above or below 0.5 depends on the size of the $B\,^2\Sigma_{1/2}$ state binding energy compared to the fine-structure splitting. Particular final-state selectivity is found in the vicinity of the near-red-wing satellites and in the near blue wings. For the Na$\mathscr{R}$ molecules at least, then, substantial selectivity in product formation may be achieved, even for weak radiation fields and for states separated by much less than the average collision energy. The satellite regions, with their relatively large absorption coefficients, spectral localization, and large branching ratios appear promising for the study of product selectivity in other types of scattering processes.

ACKNOWLEDGMENT

This work was supported by the National Science Foundation under Grant No. PHY-8509881.

[1]P. Thomann, K. Burnett, and J. Cooper, Phys. Rev. Lett. **45**, 1325 (1980).
[2]K. Burnett, J. Cooper, R. J. Ballagh, and E. W. Smith, Phys. Rev. A **22**, 2005 (1980).
[3]K. Burnett and J. Cooper, Phys. Rev. A **22**, 2027, 2044 (1980).
[4]V. Kroop and W. Behmenberg, Z. Phys. A **294**, 299 (1980).
[5]W. J. Alford, K. Burnett, and J. Cooper, Phys. Rev. A **27**, 1310 (1983).
[6]M. D. Havey, G. E. Copeland, and W. J. Wang, Phys. Rev. Lett. **50**, 1767 (1983).
[7]N. Bowering, T. D. Raymond, and J. W. Keto, Phys. Rev. Lett. **52**, 1880 (1984).
[8]P. S. Julienne, Phys. Rev. A **26**, 3299 (1982).
[9]P. S. Julienne, in *Proceedings of the Sixth International Conference on Spectral Line Shapes, Boulder, Colorado, 1982,* edited by K. Burnett (de Gruyter, Berlin, 1982).
[10]K. C. Kulander and F. Rebentrost, Phys. Rev. Lett. **51**, 1262 (1983).
[11]K. C. Kulander and F. Rebentrost, J. Chem. Phys. **80**, 5623 (1984).
[12]K. Burnett, Comments At. Mol. Phys. **13**, 179 (1983).
[13]W. J. Alford, N. Anderson, K. Burnett, and J. Cooper, Phys. Rev. A **30**, 2366 (1984).
[14]M. D. Havey and L. L. Vahala, in *Proceedings of the Seventh International Conference on Spectral Line Shapes, Aussois, France, 1984,* edited by F. Rostas (de Gruyter, Berlin, 1984).
[15]J. Vigue, J. A. Beswick, and M. Broyer, J. Phys. (Paris) **44**, 1225 (1983).
[16]S. Singer, K. Freed, and Y. B. Band, J. Chem. Phys. **77**, 1942 (1982).
[17]U. Fano, J. Opt. Soc. Am. **65**, 979 (1975).
[18]J. T. Hougen, Natl. Bur. Stand. (U.S.) Monograph No. 115, Natl. Bur. Stand. Institute for Basic Standards (U.S. GPO, Washington, D.C., 1970).
[19]G. Herzberg, *Spectra of Diatomic Molecules,* 2nd ed. (Van Nostrand Reinhold, New York, 1950).
[20]Preliminary results of our work are reported in M. D. Havey, G. E. Copeland, and W. J. Wang, Phys. Rev. Lett. **50**, 1767 (1983); and in M. D. Havey and L. L. Vahala in Ref. 14.
[21]The potentials shown are taken from R. P. Saxon, R. E. Olson, and B. Liu, J. Chem. Phys. **67**, 2692 (1977), with the electronic-spin-orbit Hamiltonian diagonalized to give Fig. 1.
[22]R. E. M. Hedges, D. L. Drummond, and A. Gallagher, Phys. Rev. A **6**, 1519 (1972).
[23]W. Behmenberg, V. Kroop, and F. Rebentrost, J. Phys. B **18**, 2693 (1985).
[24]L. L. Vahala, P. S. Julienne, and M. D. Havey, Phys. Rev. A **34**, 1856 (1986).
[25]L. C. Balling, J. J. Wright, and M. D. Havey, Phys. Rev. A **26**, 1426 (1982).
[26]B. P. Kibble, G. Copley, and L. Krause, Phys. Rev. **153**, 9 (1967).
[27]G. York, R. Scheps, and A. Gallagher, J. Chem. Phys. **63**, 1052 (1975).
[28]M. D. Havey, S. E. Frolking, and J. J. Wright, Phys. Rev. Lett. **45**, 1783 (1980); W. P. Lapatovich, R. Ahmad-Bitar, P. E. Moskowitz, I. Renhorn, R. Gottscho, and D. E. Pritchard, J. Chem. Phys. **73**, 5419 (1980).
[29]M. D. Havey, S. E. Frolking, J. J. Wright, and L. C. Balling, Phys. Rev. A **24**, 3105 (1981).
[30]For effects on fine-structure transitions, see L. Krause, in *The Excited State in Chemical Physics* (Wiley, New York, 1975).
[31]C. H. Greene and R. N. Zare, Annu. Rev. Phys. Chem. **33**, 119 (1982).
[32]P. S. Julienne and F. H. Mies, Phys. Rev. A **30**, 831 (1984).
[33]E. Czuchaj and J. Sienkiewicz, Z. Naturforsch., Teil A **34**, 694 (1979).
[34]J. Pascale, Phys. Rev. A **28**, 632 (1983).
[35]M. Philippe, F. Masnou-Seeuws, and P. Valiron, J. Phys. B **12**, L493 (1979).
[36]W. P. West and A. Gallagher, Phys. Rev. A **17**, 1431 (1978).
[37]M. J. Jongerius, T. Hollander, and C. Th. Alkemade, J. Quant. Spectrosc. Radiat. Transfer **26**, 285 (1981).
[38]J. Apt and D. E Pritchard, J. Phys. B **12**, 83 (1979).
[39]D. F. Liao, J. F. Bjorkholm, and P. R. Berman, Phys. Rev. A **21**, 1927 (1980).